Cancer Research

Metabolic Signature Identifies Novel Targets for Drug Resistance in Multiple Myeloma

Patricia Maiso[1], Daisy Huynh[1], Michele Moschetta[1], Antonio Sacco[1], Yosra Aljawai[1], Yuji Mishima[1], John M. Asara[2], Aldo M. Roccaro[1], Alec C. Kimmelman[3], and Irene M. Ghobrial[1]

Abstract

Drug resistance remains a major clinical challenge for cancer treatment. Multiple myeloma is an incurable plasma cell cancer selectively localized in the bone marrow. The main cause of resistance in myeloma is the minimal residual disease cells that are resistant to the original therapy, including bortezomib treatment and high-dose melphalan in stem cell transplant. In this study, we demonstrate that altered tumor cell metabolism is essential for the regulation of drug resistance in multiple myeloma cells. We show the unprecedented role of the metabolic phenotype in inducing drug resistance through LDHA and HIF1A in multiple myeloma, and that specific inhibition of LDHA and HIF1A can restore sensitivity to therapeutic agents such as bortezomib and can also inhibit tumor growth induced by altered metabolism. Knockdown of LDHA can restore sensitivity of bortezomib resistance cell lines while gain-of-function studies using LDHA or HIF1A induced resistance in bortezomib-sensitive cell lines. Taken together, these data suggest that HIF1A and LDHA are important targets for hypoxia-driven drug resistance. Novel drugs that regulate metabolic pathways in multiple myeloma, specifically targeting LDHA, can be beneficial to inhibit tumor growth and overcome drug resistance. *Cancer Res; 75(10); 2071–82. ©2015 AACR.*

Introduction

Cellular metabolic versatility is essential for the maintenance of energy production throughout a range of oxygen concentrations (1). Metabolic changes occurring in cancer cells are considered to be fundamental for the transformation of normal cells into cancer cells. A common property of invasive cancers is an altered glucose metabolism or glycolysis (1). Glycolysis converts glucose into pyruvate and in normal cells, this process is inhibited by the presence of oxygen, which allows mitochondria to oxidize pyruvate to CO_2 and H_2O. This inhibition is termed as the "Pasteur effect" (2). Conversion of glucose to lactic acid in the presence of oxygen is known as aerobic glycolysis or the "Warburg effect" and the increase of aerobic glycolysis is often observed in tumor cells (3–5).

One of the most recognized reasons for altered tumor metabolism is hypoxia in the tumor microenvironment (6, 7). Cells respond to the hypoxic microenvironment with the activation of hypoxia-inducible factor 1 (HIF1) transcription factor. The net result of hypoxic HIF1 activation is to shift energy production by increasing glycolysis and decreasing mitochondrial function (6). The largest functional group of genes consistently regulated by HIF1 is associated with glucose metabolism. HIF1 increases the expression of the glucose transporters, enzymatic breakdown of glucose into pyruvate and enzymes involved in the pyruvate metabolism as well as lactate production (8, 9). Although HIF1 was initially identified because of its response to low O_2 concentrations, it is now apparent that HIF1 can be regulated by other factors such as oncogene activation (*RAS*, *MYC*, and *PI3K*) or loss of tumor suppressors, including *VHL* (von Hippel–Lindau) or *PTEN*, leading to increased glycolysis, angiogenesis, and drug resistance (10–12).

Multiple myeloma is an incurable plasma cell cancer selectively localized in the bone marrow. The introduction of novel agents, including bortezomib in combination with autologous stem cell transplantation, has led to a significant advancement in the treatment of patients, leading to complete response in many patients. Unfortunately, most patients ultimately relapse due to the presence of surviving tumor cells at the minimal residual disease (MRD) state, suggesting the presence of drug resistance within specific niches in the bone marrow. The bone marrow has heterogeneous areas of hypoxia and these specific niches are altered during chemotherapy and radiotherapy (1). We hypothesize that hypoxia in specific bone marrow niches regulates the maintenance of MRD cells that are resistant to treatment and have the capability to induce relapse. We sought to investigate the mechanism underlying this drug resistance through the cellular metabolic profile of multiple myeloma cells in normoxic and hypoxic conditions. Our results reveal unprecedented features of multiple myeloma cells metabolism and further demonstrate that LDHA and HIF1A are valid targets to prevent multiple myeloma drug resistance and progression *in vivo*.

[1]Medical Oncology, Dana-Farber Cancer Institute and Harvard Medical School, Boston, Massachusetts. [2]Division of Signal Transduction, Beth Israel Deaconess Medical Center, Boston, Massachusetts. [3]Division of Genomic Stability and DNA Repair, Department of Radiation Oncology, Dana-Farber Cancer Institute, Boston, Massachusetts.

Note: Supplementary data for this article are available at Cancer Research Online (http://cancerres.aacrjournals.org/).

Corresponding Author: Irene M. Ghobrial, Dana-Farber Cancer Institute, Harvard Medical School, 450, Brooklyn Avenue, Boston, MA 02115. Phone: 617-632-4198; Fax: 617-582-8606; E-mail: irene_ghobrial@dfci.harvard.edu

doi: 10.1158/0008-5472.CAN-14-3400

Materials and Methods

Cells

Multiple myeloma cell lines MM1S, H929, and RPMI8226 (were kindly provided by Prof. Jesús F. San Miguel, Clinica Universidad de Navarra, Pamplona, Spain). Cell lines were cultured in RPMI1640 medium with L-glutamine and supplemented with antibiotics (penicillin at 100 U/mL, streptomycin at 100 μg/mL) and 10% FBS. The luciferase (luc)-expressing MM1S-GFP/luc cell lines were generated by retroviral transduction with the pGC-gfp/luc vector (kind gift of Dr. A. Kung, Dana-Farber Cancer Institute, Boston, MA).

Growth inhibition assay

The inhibitory effect of different drugs was assessed by measuring MTT (Chemicon International) dye absorbance, as previously described (13, 14).

Cell cycle and apoptosis assays

Cell-cycle analysis was profiled by flow cytometry using propidium iodide (PI) staining (5 μg/mL, Sigma Chemical) after 24 hours culture in normoxic or hypoxic conditions. Apoptosis was measured using Annexin V–FITC staining and flow cytometric analysis according to the manufacturer's protocol.

Gene expression profile

Gene expression profile has been performed on MM1S using Affymetrix Human Genome U133 Plus 2.0 Array, (GEO accession number: GSE52315). Comparison between normoxia ($n = 3$) and hypoxia ($n = 3$) was performed by using dChip (2-fold change; $P < 0.05$). Differentially expressed genes were classified using dChip software. Gene Set Enrichment Analysis (GSEA) was performed using the publicly available desktop application from the Broad Institute (http://www.broad.mit.edu/gsea/software/software_index.html). The gene sets database used was that of functional sets, s2.symbols.gmt. *P* values were calculated by permuting the genes 1,000 times. The classic enrichment statistic was selected. The gene expression datasets from Schaefer CF and colleagues provided in the Pathway Interaction Database (NCI and Nature Publishing Group) were used for HIF1A and HIF2A analysis in GSEA (15). The gene expression datasets REACTOME_ GLUCOSE_ METABOLISM and KEGG_ PYRUVATE_ METABOLISM were used, respectively, for glucose metabolism and TCA cycle analysis in GSEA. Gene pattern (http://www.broadinstitute.org/cancer/software/genepattern/download) analysis was performed using the "Comparative Marker Selection" tool to find the genes that are most closely correlated with the two phenotypes normoxia and hypoxia.

To determine the gene enrichments sets of hypoxia-related pathways, glucose metabolism, and TCA cycle in plasma cells isolated from normal subjects or from newly diagnosed multiple myeloma patients, as well as from responder and relapsed patients to bortezomib, we used published datasets from the Gene Expression Omnibus by Chng and colleagues and Mulligan and colleagues (series numbers GSE6477 and GSE9782, respectively; refs. 16, 17).

Metabolite profiling

Metabolites were extracted in ice-cold methanol and endogenous metabolite profiles were obtained using two liquid chromatography-tandem mass spectrometry (LC-MS) methods as described (18). Data were acquired using a 5500 QTRAP triple quadrupole mass spectrometer (AB/Sciex) coupled to a Prominence UFLC system (Shimadzu) via selected reaction monitoring of a total of 289 endogenous water soluble metabolites for steady-state analyses of samples.

Metaboanalyst software was used for analysis. Metabolite levels were normalized to the total of all metabolites detected on a triplicate set of cells treated identically to the experimental cells.

Hexokinase activity and lactate measurement

Hexokinase activity was measured with the Hexokinase Assay Kit (Abcam) and cellular lactate levels were measured using the Lactate Colorimetric Assay Kit (Biovision) according to the manufacturer's instructions.

RNA purification, reverse transcription, and quantitative RT-PCR

Total RNA was prepared with QIAzol reagent (Invitrogen) according to the manufacturer's instructions. One microgram of total RNA was reverse transcribed using SuperScript III First-Strand Synthesis (Invitrogen). Diluted cDNAs were analyzed by real-time PCR using SYBR Green I Master Mix on Lightcycler 480 (Roche) on an ABI Prism 7900 Fast instrument. The level of gene expression was normalized to 18S. The primer sequences are provided in Table 1.

In vivo studies

Six-week-old female SCID-beige mice from Charles River Laboratories were i.v. implanted with 100 μL of 5×10^6 MM1S-GFP/luc-scramble, MM1S-GFP/luc-shHIF1A, or MM1S-GFP/luc-shLDHA. Mice were treated with bortezomib, 0.75 mg/kg in PBS once weekly by intraperitoneal injection beginning 10 days after tumor implantation until moribund. Mice with different stages of tumor development based on tumor size detected by bioluminescence (BLI) were treated with the hypoxia marker pimonidazole hydrochloride (PIMO; 100 mg/kg by intraperitoneal injection; Hypoxyprobe Store). After 4 hours, bone marrow was isolated from one femur by flushing with cold PBS and prepared for RNA isolation as described, the other femur was used for IHC.

In vivo tumor growth has been assessed by using *in vivo* bioluminescence imaging. Mice were injected with 75 mg/kg of luciferin (Xenogen), and tumor growth was detected by bioluminescence 3 minutes after the injection, using Xenogen In Vivo Imaging System (Caliper Life Sciences). Mice were monitored and sacrificed when they developed side effects of tumor burden in accordance with approved protocol of the Dana-Farber Cancer Institute (DFCI, Boston, MA) Animal Care and Use Committee.

Immunohistochemistry

In the *in vivo* model, femurs were fixed in 4% paraformaldehyde and embedded in paraffin. Sections were stained with hematoxylin

Table 1. Primer sequences

Gene	Primers
human *HIF1A*	F: TTGGACACTGGTGGCTCATTAC
	R: TGAGCTGTCTGTGATCCAGCAT
human *HIF2A*	F: GTGTTGTGGACACTGCAGACTTGT
	R: ATGACTCCACTGCTCGGATTGTCA
human *HK2*	F: AGCCCTTTCTCCATCTCCTT
	R: AACCATGACCAAGTGCAGAA
human *LDHA*	F: GGAGATCCATCATCTCTCC
	R: GGCCTGTGCCATCAGTATCT
human *18S*	F: TCAACTTTCGATGGTAGTCGCCGT
	R: TCCTTGGATGTGGTAGCCGTTTCT

and eosin (H&E) in accordance with standard procedures. Immunohistochemistry was performed using antibodies against Mab1 (Hypoxyprobe Store), HK2 (Cell Signaling Technology) and LDHA (Cell Signaling Technology) according to the manufacturer's instructions. All multiple myeloma biopsies were evaluated at DFCI and the histologic diagnosis was based on H&E. Histologic IHC images were obtained with the Olympus AH2 microscope camera from Center Valley. Image acquisition and processing software were performed using an Olympus DP12 camera and software.

Knockdown constructs

Stable knockdowns of HIF1A, HIF2A, HK2, and LDHA were generated by lentiviral transduction of MM1S and MM1S-GFP/luc cells with five independent shRNA hairpin sequences targeting human HIF1A, HIF2A, HK2, and LDHA, respectively. A scrambled shRNA sequence was used as control (TRCN0000072212).

Lentiviral shRNAs were obtained from The RNAi Consortium (TCR) collection of the Broad Institute (Cambridge, MA). The TCR numbers for the shRNA used are found in Table 2.

Statistical analysis

P values described in the *in vitro* assays are based on *t* tests (two-tailed; α 0.05). *P* values are provided for each figure.

Results

Hypoxia promotes drug resistance in multiple myeloma

We first examined hypoxia-regulated pathways in primary multiple myeloma patients to test the enrichment of HIF1A and HIF2A (15) pathways in plasma cells isolated from bone marrow of normal donors and multiple myeloma patients; we analyzed the published gene expression datasets (series numbers, GSE6477 and GSE9782, respectively; refs. 16, 17). Newly diagnosed multiple myeloma patients showed an enrichment of HIF1A and HIF2A pathways compared with normal donors (Supplementary Fig. S1A), we also found an enrichment of both pathways in patients with relapsed and bortezomib-refractory myeloma compared with patients responding to bortezomib (Supplementary Fig. S1B).

We next investigated whether hypoxia plays a role in drug resistance in multiple myeloma. Given the importance of hypoxia in facilitating tumor progression and resistance to chemotherapy in solid tumors, we evaluated the effect of several conventional agents used in the treatment of multiple myeloma such as dexamethasone, melphalan, and bortezomib, either under normoxia (20% O_2) or hypoxia (1% O_2) in multiple myeloma cells. Our findings indicate that hypoxia inhibited the effect of bortezomib and melphalan in MM1S (Supplementary Fig. S1C), RPMI8226 (Supplementary Fig. S1D), and H929 (Supplementary Fig. S1E) cells. As hypoxia has been shown to cause cell-cycle arrest and this could potentially impact therapeutic responses, we analyzed the effect of hypoxia on cell-cycle regulation and apoptosis by flow cytometry. After 24 hours, hypoxia induced G_1 arrest (Supplementary Fig. S1F) but not apoptosis (Supplementary Fig. S1G) in multiple myeloma cells. However, induction of G_1 arrest through serum starvation (Supplementary Fig. S1H) did not impact the response to bortezomib in MM1S, RPMI8226, and H929 (Supplementary Fig. S1I). Carfilzomib showed similar activity to bortezomib on MM1S, RPMI8226, and H929 cells (Supplementary Fig. S1J). Therefore, the drug resistance effect observed with hypoxia was not due to the G_1 arrest observed in hypoxic conditions. To further confirm the effect of hypoxia, we pretreated the cells for 12 hours under normoxic or hypoxic conditions and then added the therapeutic agent for an additional 24 hours under both normoxia and hypoxia. We found multiple myeloma cells responded to bortezomib treatment under normoxic conditions but not under hypoxia even with previous culture in normal oxygen levels (Supplementary Fig. S1K).

Table 2. TCR numbers for the shRNA

Gene	Clones
human *HIF1A*	TRCN0000003809
	TRCN0000003810
	TRCN0000010819
	TRCN0000318675
	TRCN0000349634
human *HIF2A*	TRCN0000003803
	TRCN0000003804
	TRCN0000003805
	TRCN0000352630
	TRCN0000342501
human *HK2*	TRCN0000037670
	TRCN0000195171
	TRCN0000196260
	TRCN0000232927
	TRCN0000232928
human *LDHA*	TRCN0000026538
	TRCN0000026536
	TRCN0000158762
	TRCN0000164922
	TRCN0000166246

Metabolic reprogramming delineates a role for drug resistance in myeloma cells

Because one of largest functional groups regulated by HIF1 is associated with glucose metabolism, we hypothesized that changes in cell metabolism could serve as the main factor of drug resistance in multiple myeloma cells. To examine mechanisms underlying metabolism-associated drug resistance, we performed targeted metabolomic profiling in MM1S cells before and after bortezomib treatment under both normoxic and hypoxic conditions. The metabolic profile of hypoxic cells demonstrated a clear shift when compared with normoxic cells; however, cells treated with bortezomib were similar to their nontreated counterparts in both conditions (Fig. 1A). In hypoxic cells, intermediates of TCA cycle and mitochondrial electron transport chain were reduced, whereas intermediates of glycolysis were elevated (Fig. 1B).

To determine specific metabolic changes are due to hypoxia and not to the G_1 cell-cycle arrest observed in hypoxic cells, we starved MM1S cells for 12 hours and the metabolic profile of MM1S cells arrested at G_1 phase showed a decrease on glucose-6-phosphate, fructose-6-phosphate, fructose-1,6-bisphosphate, pyruvate, and lactate metabolites (Fig. 1C). In contrast to G_1-arrested cells, hypoxic cells showed an increase in glycolysis metabolites, including pyruvate and lactate (Fig. 1C and D). To further examine metabolic alterations in hypoxic conditions, we performed gene expression profile (GEP) on MM1S under normoxic or hypoxic conditions and performed GSEA using the ranked gene list from Dchip (changes in gene expression greater than 2-fold with *P* value lower than 0.05 were considered significant). To identify the most significant pathways altered by hypoxia, we compared normoxic samples ($n = 3$) versus hypoxic samples ($n = 3$) and found that after 24 hours of hypoxia, 3,609 genes were deregulated (1,649 genes were upregulated in hypoxia and 1,960 genes were upregulated in normoxia; Fig. 2A). The main pathways altered by hypoxic culture

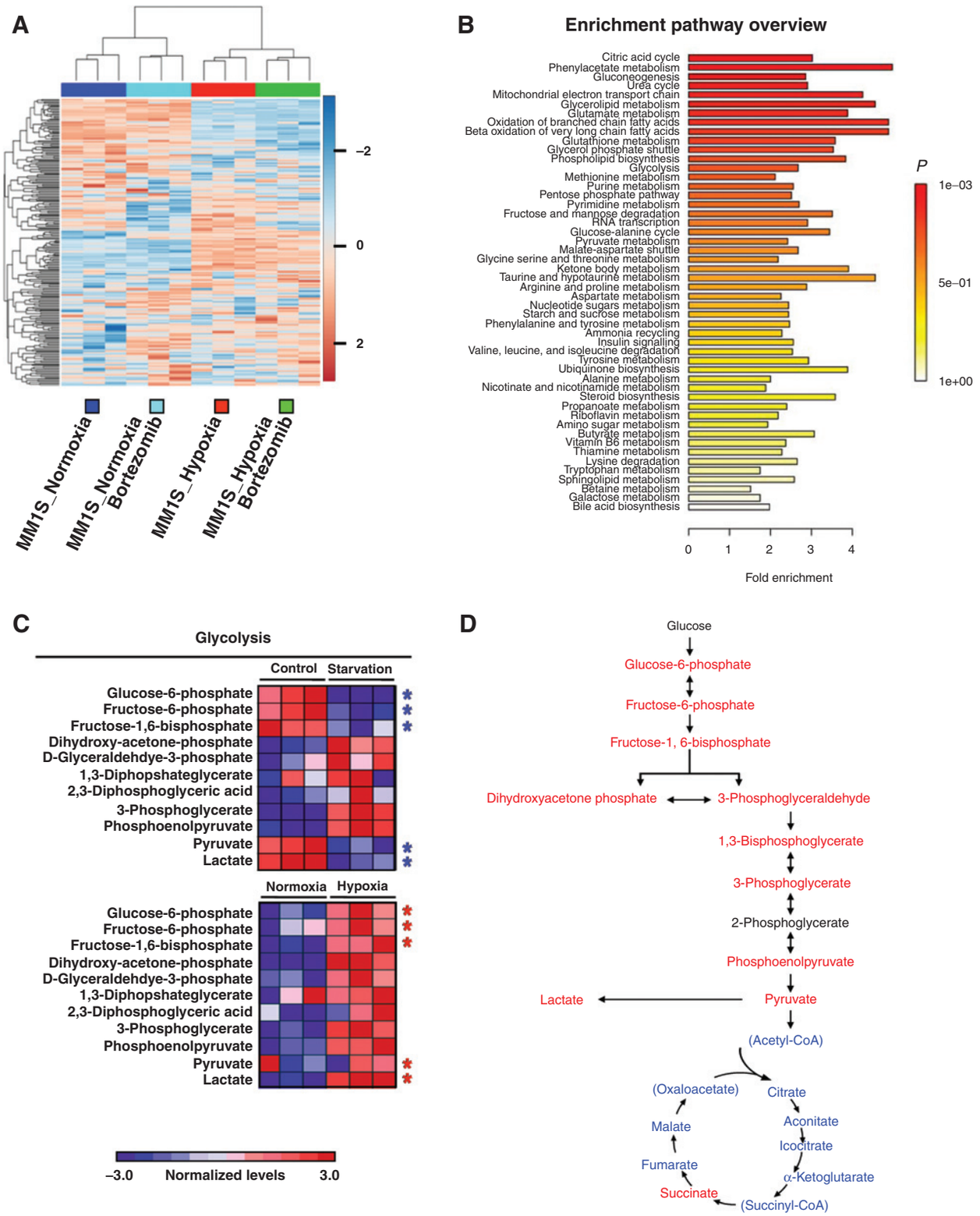

Figure 1.
Metabolic profiles of multiple myeloma (MM) cells reflect an increase in glycolysis in response to hypoxia. A, unsupervised hierarchical clustering was performed using the 289 metabolites whose intensity varied across the 12 samples. Samples were clustered using Metaboanalyst software. For each metabolite, data were median centered (white), with the lowest and highest intensity values in blue and red, respectively. B, metabolite enrichment pathway overview. C, heatmap comparing relative levels of metabolites on multiple myeloma cells in response to serum starvation for 12 hours and to hypoxia for 24 hours. Heatmaps show the relative levels of starved cells (top) and hypoxic cells (bottom) in comparison with MM1S-control-normoxic cells. D, schema illustrating the specific metabolites that are increased (red) or decreased (blue) in multiple myeloma cells in response to hypoxia after 24 hours.

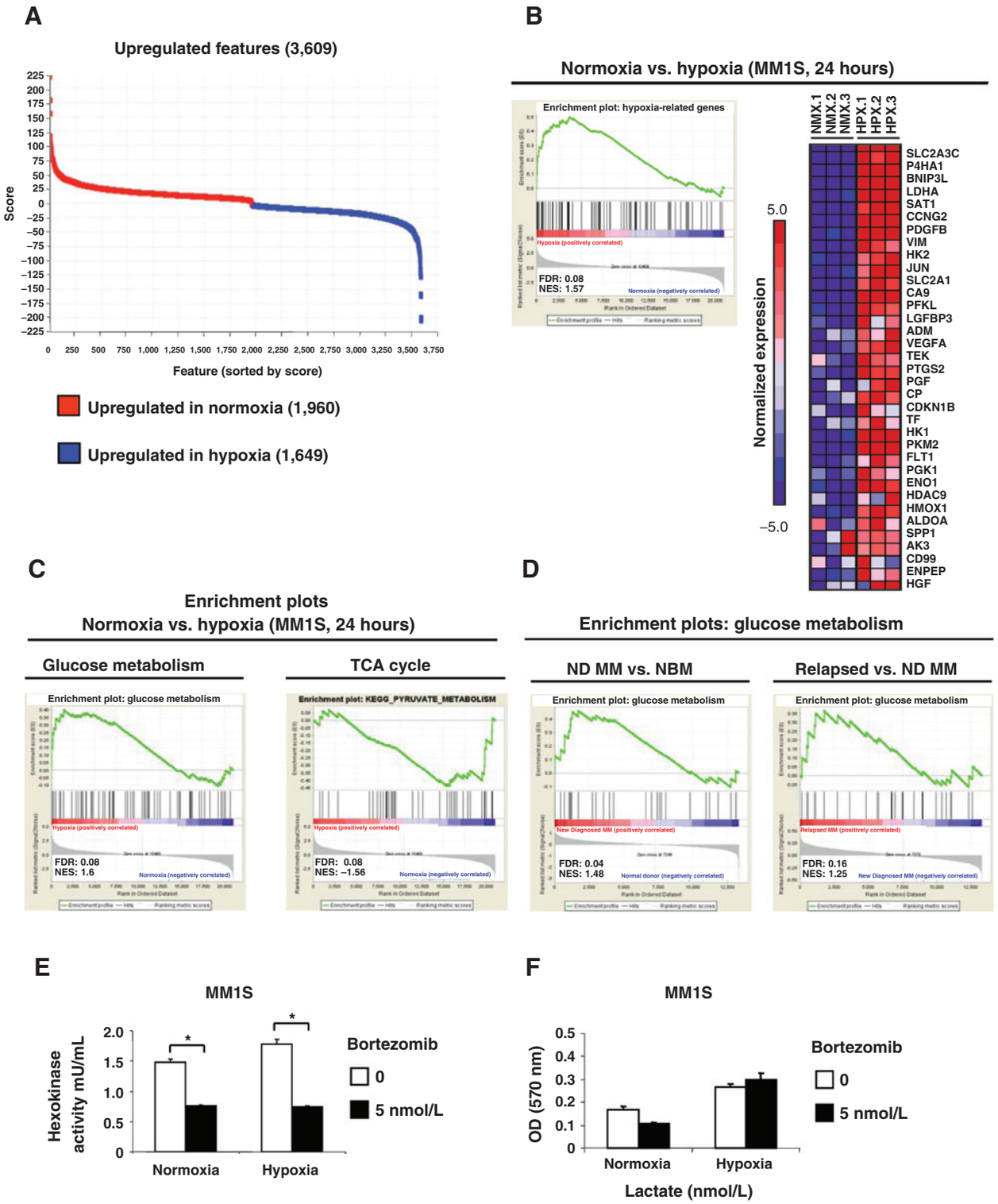

Figure 2.
GEPs evidence an increase in glycolytic and lactate enzymes in response to hypoxia. A, gene pattern comparative marker showing upregulated genes in normoxic and hypoxic multiple myeloma (MM) cells; $n = 3$ samples in each condition. B, microarray data were analyzed using GSEA software to identify functionally related groups of genes (gene sets) with statistically significant enrichment. The figure shows the enrichment plot and the top 35 enriched genes for hypoxia-related set. NMX, normoxia; HPX, hypoxia. C, GSEA enrichment plots for glucose metabolism and TCA cycle in normoxia versus hypoxia conditions in multiple myeloma cells. D, GSEA enrichment plots for glucose metabolism and TCA cycle in newly diagnosed (ND) patients versus normal bone marrows (NBM; GSE6477) and in relapsed versus newly diagnosed (ND) myeloma patients (GSE9782). E, hexokinase activity in MM1S cells treated with bortezomib (5 nmol/L) under normoxic and hypoxic conditions for 24 hours. F, lactate levels in MM1S cells treated with bortezomib (5 nmol/L) under normoxic and hypoxic conditions for 24 hours. *, $P < 0.05$; **, $P < 0.005$; and ***, $P < 0.0005$. FDR, false discovery rate.

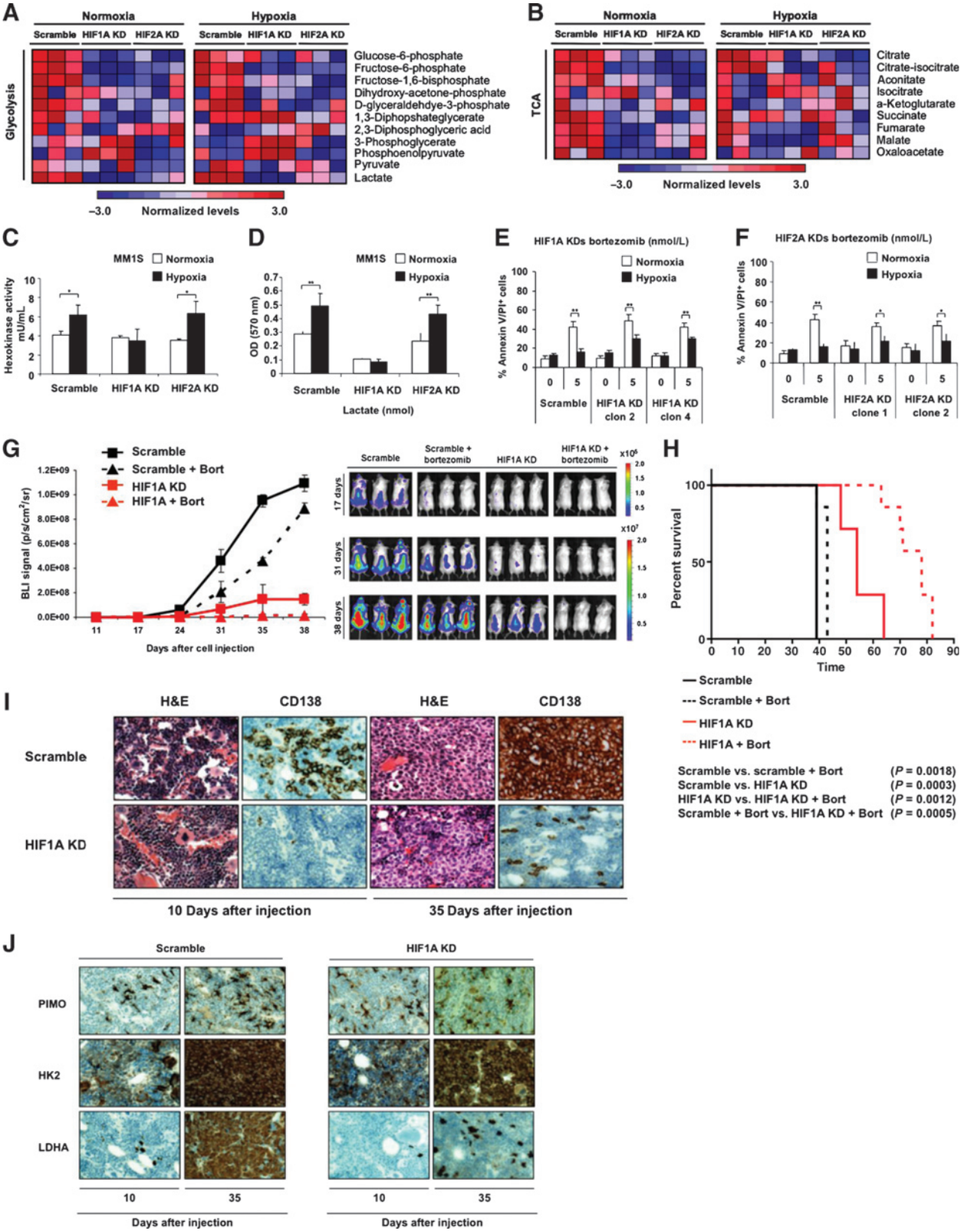
A
Normoxia
Hypoxia
Scramble
HIF1A KD
HIF2A KD
Glycolysis
Glucose-6-phosphate
Fructose-6-phosphate
Fructose-1,6-bisphosphate
Dihydroxy-acetone-phosphate
D-glyceraldehdye-3-phosphate
1,3-Diphopshateglycerate
2,3-Diphosphoglyceric acid
3-Phosphoglycerate
Phosphoenolpyruvate
Pyruvate
Lactate
–3.0
Normalized levels
3.0
B
TCA
Citrate
Citrate-isocitrate
Aconitate
Isocitrate
a-Ketoglutarate
Succinate
Fumarate
Malate
Oxaloacetate
C
MM1S
Normoxia
Hypoxia
Hexokinase activity mU/mL
D
OD (570 nm)
Lactate (nmol)
E
HIF1A KDs bortezomib (nmol/L)
% Annexin V/PI+ cells
HIF1A KD clon 2
HIF1A KD clon 4
F
HIF2A KDs bortezomib (nmol/L)
HIF2A KD clone 1
HIF2A KD clone 2
G
Scramble
Scramble + Bort
HIF1A KD
HIF1A + Bort
BLI signal (p/s/cm²/sr)
Days after cell injection
Scramble + bortezomib
HIF1A KD + bortezomib
17 days
31 days
38 days
H
Percent survival
Time
Scramble
Scramble + Bort
HIF1A KD
HIF1A + Bort
Scramble vs. scramble + Bort (P = 0.0018)
Scramble vs. HIF1A KD (P = 0.0003)
HIF1A KD vs. HIF1A KD + Bort (P = 0.0012)
Scramble + Bort vs. HIF1A KD + Bort (P = 0.0005)
I
H&E
CD138
Scramble
HIF1A KD
10 Days after injection
35 Days after injection
J
PIMO
HK2
LDHA
10
35
Days after injection

were those involved in glucose metabolism (including glycolytic enzymes; Fig. 2B and C) and TCA cycle (Fig. 2C). We also validated our data on additional cell lines, and showed that similar changes on key metabolic genes (HK2, PFKFB3, PFKFB4, and LDHA) were observed among all the cell lines tested MM1S, H929, and RPMI8226 (Supplementary Fig. S2A–S2C).

Glucose metabolism gene set was also enriched in the datasets comparing plasma cells from newly diagnosed multiple myeloma patients with normal donors and in plasma cells from relapsed myeloma patients versus newly diagnosed (ND) multiple myeloma (Fig. 2D).

Importantly, hypoxia regulates expression of HIF1A target genes that are critical for increased glucose uptake and catabolism such as hexokinase II (*HK2*) and lactate dehydrogenase A (*LDHA*; refs. 19–21). Both genes were significantly upregulated in our expression datasets (FC = 2.1 and FC = 5.2, respectively). To test whether bortezomib affects the enzymatic activities of HK2 and LDHA, we measured the hexokinase and lactate activities in cells treated with bortezomib under normoxic and hypoxic conditions. Bortezomib was able to decrease the hexokinase activity even under hypoxic conditions (Fig. 2E) but not the lactate activity that was significantly increased under hypoxic conditions (Fig. 2F). We found that bortezomib inhibited HK2 activity of multiple myeloma cells under hypoxic conditions but not lactate activity, suggesting that LDHA may play a role in modulating drug resistance of multiple myeloma cells in hypoxia.

HIF1A knockdown decreases lactate levels and partially restores the effect of bortezomib under hypoxic conditions

HIF1A is the main pathway to induce glycolysis and lactate production during hypoxia (20, 22, 23). Under low oxygen conditions, HIF1A is stabilized and promotes transcription of several genes critical for the cellular response to hypoxia (10). We hypothesized that cells lacking HIF1A will fail to upregulate glycolytic enzymes and lactate production in response to hypoxia and will render them more sensitive to chemotherapy. To test this hypothesis, we performed HIF1A and HIF2A loss-of-function studies in multiple myeloma cells. HIF1A and HIF2A knockdown efficiencies were evaluated using qRT-PCR and Western blot analysis (Supplementary Fig. S3A–S3C). The metabolic profile of MM1S-HIF1A knockdown cells demonstrated a clear shift away from glycolytic metabolism when compared with MM1S-scramble under normoxic conditions (Fig. 3A), and a similar shift occurred under hypoxic conditions (Fig. 3A). In MM1S- HIF2A knockdown, intermediates of glycolysis were slightly reduced, but pyruvate and lactate levels increased after hypoxia exposure (Fig. 3A). The levels of TCA cycle intermediates decreased in HIF1A and HIF2A knockdowns compared with MM1S-scramble after either normoxia or hypoxia exposures (Fig. 3B).

To confirm that the HIF1A and HIF2A knockdown metabolites patterns reflected a shift in glycolysis and mainly in lactate production, we measure hexokinase activity and lactate production in both cells under normoxic and hypoxic conditions. As expected, HIF1A knockdown cells showed a reduction in hexokinase activity under hypoxic conditions similar to normoxic levels (Fig. 3C) and a significant decrease in lactate production in both normoxic and hypoxic levels compared with the scramble (Fig. 3D). Hexokinase and lactate activities did not change in HIF2A knockdown cells (Fig. 3C and D).

Consistent with the metabolite profile pattern and the reduction of hexokinase and lactate levels, the HIF1A knockdown partially overcomes drug resistance to bortezomib (Fig. 3E) and melphalan (Supplementary Fig. S3D) after hypoxia exposure. However, HIF2A knockdown did not produce similar results, indicating that HIF2A is not essential for the induced drug resistance (Fig. 3F).

To determine the *in vivo* effect of HIF1A loss, we knock down HIF1A expression in MM1S-GFP/luc. HIF1A knockdown efficiency was evaluated by qRT-PCR (Supplementary Fig. S3E). MM1S-GFP/luc-scramble ($n = 14$) and MM1S-GFP/luc-shHIF1A (HIF1A knockdown, clone 2; $n = 14$) were injected i.v. into NOD-SCID mice. After 10 days we started the treatment of each group ($n = 7$ per group), 28 mice were treated with vehicle ($n = 14$) or bortezomib (0.75 mg/kg, weekly, intraperitoneally; $n = 14$). Tumor growth was measured using luciferin and BLI.

After 35 days, the scramble group demonstrated significant tumor progression, whereas minimal tumor growth was detected in mice injected with HIF1A knockdown (Fig. 3G). Mice groups injected with scramble cells and treated with bortezomib showed a delay in tumor growth, but after 35 days, the tumor growth increased reaching similar BLI signal to the control group (Fig. 3G). Bortezomib showed a significant effect in the HIF1A knockdown group (Fig. 3G), increasing the survival significantly compared with the nontreated group and compared with the control group treated with bortezomib (Fig. 3H). Furthermore, mice femurs were collected at day 10 and at day 35, and CD138 expression was analyzed by IHC. In concordance with our BLI data, we observed an increase of $CD138^+$ population with a strong staining in the scramble biopsies, whereas the HIF1A knockdown group remained very low even at day 35 (Fig. 3I). The hypoxic state of multiple myeloma cells in the bone marrow was also examined by intraperitoneal injection of pimonidazole (PIMO) before bone marrow isolation and IHC was performed to detect HK2 and LDHA protein levels in tumor cells. Our results demonstrate that

Figure 3.

Stable knockdown of HIF1 decreases lactate levels and partially restores the effect of bortezomib under hypoxic conditions. A and B, heatmap comparing metabolite patterns of HIF1A and HIF2A knockdowns (KD) in normoxia and hypoxia. A, glycolysis; B, TCA cycle. Red and blue indicate up- or downregulation, respectively. Scramble, HIF1A, and HIF2A knockdowns ($n = 12$) were cultured in 20% O_2 (normoxia) or 1% O_2 (hypoxia) for 24 hours, and metabolites were analyzed by LC-MS. C, hexokinase activity of HIF1A and HIF2A knockdowns under normoxic and hypoxic conditions, normalized to scramble in normoxia. D, lactate levels in HIF1A and HIF2A knockdowns under normoxic and hypoxic conditions, normalized to scramble in normoxia. E and F, MM1S scramble, HIF1A (E) and HIF2A (F) knockdowns were incubated with bortezomib (5 and 10 nmol/L) under normoxic or hypoxic conditions for 24 hours and apoptosis was evaluated by Annexin V/PI staining and flow cytometric analysis. Graphs and bars represent the mean ± SD for cell apoptosis in three independent experiments performed in four replicates. Two clones of each knockdown were tested for apoptosis assays. G, mice were i.v. injected with 5×10^6 of MM1S-GFP/luc scramble or MM1S-GFP/luc-shHIF1A. Vehicle or bortezomib were administered intraperitoneally, weekly, at 0.75 mg/kg, starting 10 days after injection and xenograft growth was tested by BLI. H, Kaplan–Meier curve comparing survival of different groups. I, histopathology was performed on different groups 10 and 35 days after injection. H&E and CD138 staining were detected by IHC. J, histopathology was performed on different groups 10 and 35 days after injection. PIMO, HK2, and LDHA staining were detected by IHC.

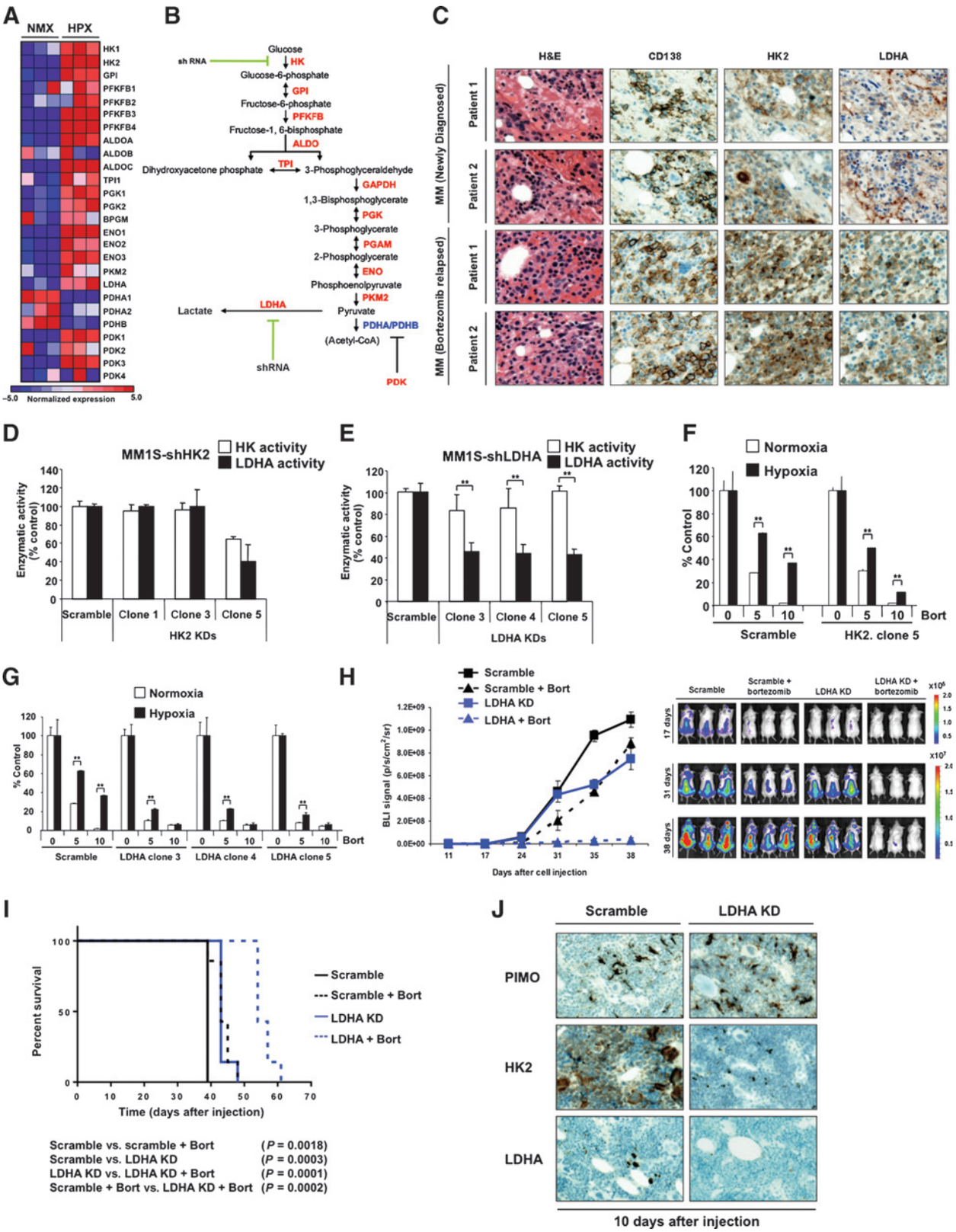
A
NMX
HPX
HK1
HK2
GPI
PFKFB1
PFKFB2
PFKFB3
PFKFB4
ALDOA
ALDOB
ALDOC
TPI1
PGK1
PGK2
BPGM
ENO1
ENO2
ENO3
PKM2
LDHA
PDHA1
PDHA2
PDHB
PDK1
PDK2
PDK3
PDK4
−5.0 Normalized expression 5.0
B
sh RNA
Glucose
HK
Glucose-6-phosphate
GPI
Fructose-6-phosphate
PFKFB
Fructose-1, 6-bisphosphate
ALDO
TPI
Dihydroxyacetone phosphate
3-Phosphoglyceraldehyde
GAPDH
1,3-Bisphosphoglycerate
PGK
3-Phosphoglycerate
PGAM
2-Phosphoglycerate
ENO
Phosphoenolpyruvate
PKM2
LDHA
Lactate
Pyruvate
PDHA/PDHB
(Acetyl-CoA)
shRNA
PDK
C
H&E
CD138
HK2
LDHA
MM (Newly Diagnosed)
MM (Bortezomib relapsed)
Patient 1
Patient 2
Patient 1
Patient 2
D
MM1S-shHK2
HK activity
LDHA activity
Enzymatic activity (% control)
Scramble
Clone 1
Clone 3
Clone 5
HK2 KDs
E
MM1S-shLDHA
HK activity
LDHA activity
Enzymatic activity (% control)
Scramble
Clone 3
Clone 4
Clone 5
LDHA KDs
F
Normoxia
Hypoxia
% Control
Bort
Scramble
HK2. clone 5
G
Normoxia
Hypoxia
% Control
Bort
Scramble
LDHA clone 3
LDHA clone 4
LDHA clone 5
H
Scramble
Scramble + Bort
LDHA KD
LDHA + Bort
BLI signal (p/s/cm²/sr)
Days after cell injection
Scramble
Scramble + bortezomib
LDHA KD
LDHA KD + bortezomib
17 days
31 days
38 days
I
Percent survival
Time (days after injection)
Scramble
Scramble + Bort
LDHA KD
LDHA + Bort
Scramble vs. scramble + Bort (P = 0.0018)
Scramble vs. LDHA KD (P = 0.0003)
LDHA KD vs. LDHA KD + Bort (P = 0.0001)
Scramble + Bort vs. LDHA KD + Bort (P = 0.0002)
J
Scramble
LDHA KD
PIMO
HK2
LDHA
10 days after injection

the increase of the hypoxic microenvironment induces the overexpression of HK2 and LDHA in plasma cells (Fig. 3J).

Loss of LDHA sensitizes multiple myeloma cells to drug effect

To better define the functional role of glycolysis pathways in drug resistance on multiple myeloma cells, we explored the expression of the glycolytic enzymes deregulated in our genes' expression profile (GEP; Fig. 4A) and performed HK2 and LDHA loss-of-function studies on MM1S cells (Fig. 4B). HK2 and LDHA knockdown efficiency was evaluated by qRT-PCR (Supplementary Fig. S4A and S4B).

To confirm that HK2 and LDHA expression are increased in multiple myeloma, we analyzed HK2 and LDHA protein levels by IHC in plasma cells of newly diagnosed and refractory myeloma patients. Out of 20 patient samples, all samples showed high levels of HK2 and LDHA staining in tumor $CD138^+$ plasma cells (Fig. 4C). Similarly, GEP of an independent set of $CD138^+$ cells (16, 17) revealed that the expression of HK2 and LDHA increased with disease progression (Supplementary Fig. S4C).

We evaluated the effect of LDHA and HK2 knockdown on hexokinase activity and intracellular levels of lactate and found that knockdown of HK2 leads to inhibition of both hexokinase activity and lactate (Fig. 4D); however, LDHA knockdown showed a reduction in lactate but did not affect the cellular hexokinase activity compared with scramble control cells (Fig. 4E).

We next examined the effect of bortezomib in HK2 and LDHA knockdowns. MM1S-shHK2 (HK2 knockdown) cells were sensitive to the effect of bortezomib after exposure to hypoxia (Fig. 4F), whereas the effect of bortezomib was markedly higher in MM1S-shLDHA (LDHA knockdown) under both normoxic and hypoxic conditions (Fig. 4G). We also examined the effect in response to melphalan treatment, and LDHA KD restored the effect of melphalan under hypoxic conditions (Supplementary Fig. S4D). Therefore, this effect shows that metabolism-induced drug resistance represents a common mechanism of resistance to drug therapy and not just specific to bortezomib or proteasome inhibition.

LDHA expression as well as pyruvate dehydrogenase kinase 1 (PDK1) were found to be upregulated in the GEP data analysis. Both of these enzymes can limit the use of pyruvate as a carbon source for the TCA cycle (24, 25). Indeed, our metabolomics data show an overall decrease in TCA pool sizes under hypoxic conditions. To determine whether pyruvate utilization plays a role in drug resistance, we performed gain-of-function experiments with PDK1 (Supplementary Fig. S4E) and examined the effect of bortezomib in PDK1-expressing cells under normoxic conditions. We observed that MM1S-PDK1–expressing cells were resistant to the effect of bortezomib (Supplementary Fig. S4F), this effect was similar to that observed in MM1S wild-type under hypoxic conditions where PDK1 was upregulated by microarray analysis.

Similar to our previous *in vivo* studies, we knocked down LDHA expression in MM1S-GFP/luc. LDHA knockdown efficiency was evaluated by qRT-PCR (Supplementary Fig. S4G). MM1S-GFP/luc-shLDHA (LDHA knockdown, clone 4; $n = 14$) were injected i.v. into NOD-SCID mice and treatment was initiated after 10 days. Mice were treated with vehicle ($n = 7$) or bortezomib (0.75 mg/kg, weekly, intraperitoneally; $n = 7$).

After 35 days, the tumor progression was lower in the LDHA knockdown mice compared with their controls and the LDHA knockdown group treated with bortezomib showed a significant delay in tumor growth (Fig. 4H). Survival curves showed a significant difference between the scramble and LDHA knockdown groups and bortezomib highly increased the survival percentage of the LDHA knockdown mice compared with the non-treated group and with the scramble-treated group (Fig. 4I). The observed changes may be due to an impact of HIF1A and LDHA silencing on both bone marrow homing/engraftment of multiple myeloma cells, together with a reduced multiple myeloma cell growth. These data are indeed supported by the IHC studies where a reduced human-CD138 cell infiltration was documented in those mice that were injected with HIF1A- and LDHA-silenced MM1S cells compared with the related scramble control.

Mice femurs were collected at day 10 and IHC was performed to detect PIMO, HK2, and LDHA levels. In concordance with our *in vitro* data, even under hypoxic conditions as demonstrated by PIMO staining, LDHA knockdown group showed a lower HK2 expression in plasma cells (Fig. 4J).

HIF1A and LDHA expression are associated with drug resistance

To further confirm the dependence between HIF1A, LDHA, and drug resistance, we examined the relative levels of HIF1A and LDHA in a panel of six multiple myeloma representative cell lines: MM1S and MM1R (sensitive and resistant to dexamethasone), U266 and U266LR7 (sensitive and resistant to melphalan), and ANBL6 and ANBL6-bortezomib-resistant (BR; sensitive and resistant to bortezomib, respectively).

We found that HIF1A (Fig. 5A) and particularly LDHA (Fig. 5B) levels are upregulated in all the cell lines resistant to different drugs as compared with their drug-sensitive counterparts. To better characterize the role of LDHA in drug resistant to bortezomib, we knocked down LDHA expression in the bortezomib-resistant cell line ANBL6-BR (Supplementary Fig. S5A) and overexpressed HIF1A and LDHA in MM1S cells (sensitive to bortezomib; Supplementary Fig. S5B–S5D). In ANBL6-BR, LDHA knockdown restored the sensitivity to bortezomib (Fig. 5C) and in

Figure 4.

Stable loss of LDHA sensitizes multiple myeloma (MM) cells to bortezomib effect. A, heatmap comparing glycolytic enzymes expression in MM1S cells under normoxia or hypoxia. B, schematic overview of glycolytic enzymes illustrating the targeted genes. C, bone marrow biopsies from multiple myeloma patients relapsed to bortezomib treatment ($N = 20$) were fixed in Zanker formalin, embedded in paraffin blocks, and sectioned. Sections were stained for HK2 and LDHA. D, hexokinase activity and lactate production of HK2 knockdowns normalized to the scramble cells. E, hexokinase activity and lactate production of LDHA knockdowns normalized to the scramble cells. F, MM1S scramble and HK2 knockdown were incubated with bortezomib (5 and 10 nmol/L) under normoxic or hypoxic conditions for 24 hours and apoptosis was evaluated by MTT. Graphs and bars represent the mean ± SD for cell viability in three independent experiments performed in four replicates. G, MM1S scramble and LDHA knockdown were incubated with bortezomib (5 and 10 nmol/L) under normoxic or hypoxic conditions for 24 hours and apoptosis was evaluated by MTT. Graphs and bars represent the mean ± SD for cell apoptosis in three independent experiments performed in four replicates. Three clones of LDHA knockdown were tested for apoptosis assays. H, mice were i.v. injected with 5×10^6 of MM1S-GFP/luc scramble or MM1S-GFP/luc-shLDHA. Vehicle or bortezomib were administered intraperitoneally, weekly, at 0.75 mg/kg, starting 10 days after injection and xenograft growth was tested by BLI. I, Kaplan–Meier curve comparing survival of different groups. *, $P < 0.05$; **, $P < 0.005$; and ***, $P < 0.0005$. J, histopathology was performed on different groups 10 days after injection. PIMO, HK2, and LDHA staining was detected by IHC.

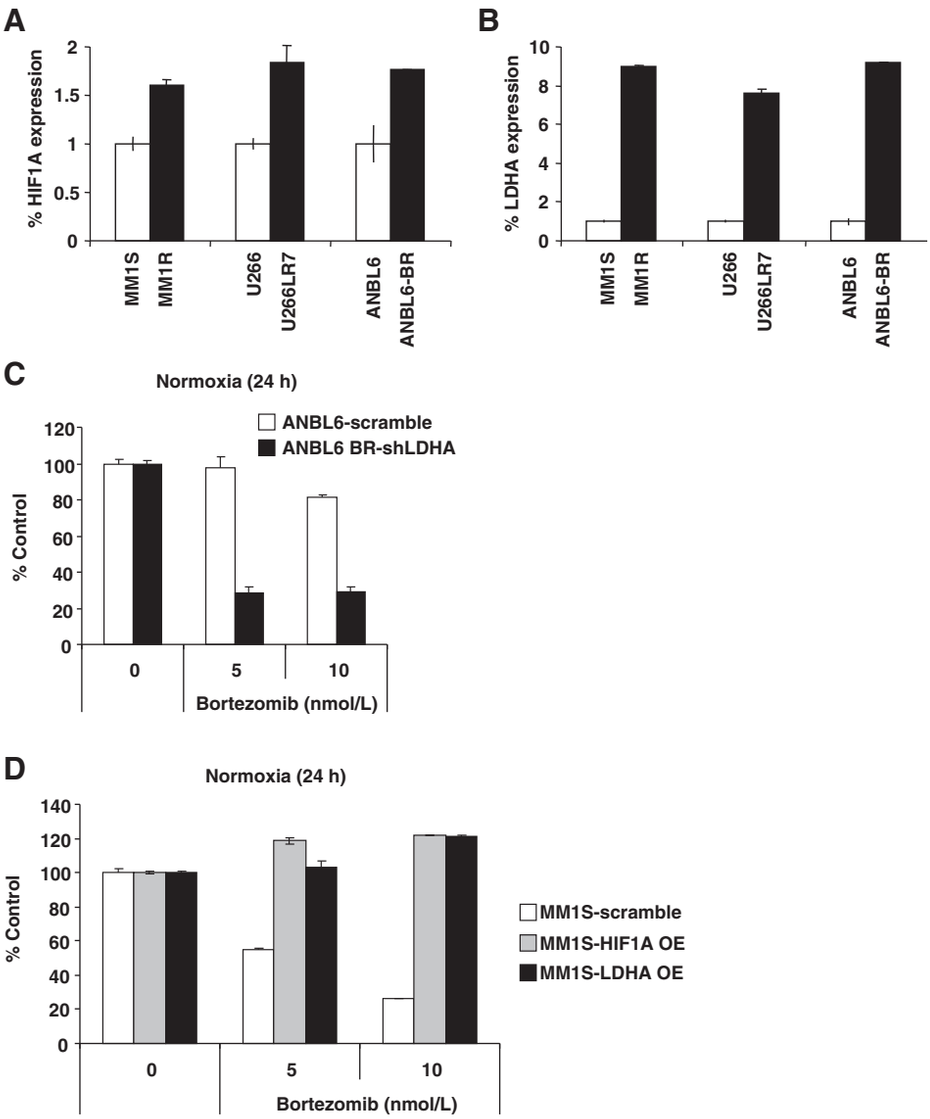

Figure 5.
HIF1A and LDHA expression are associated with drug resistance. A and B, relative mRNA levels of HIF1A (A) and LDHA (B) in MM1S and MM1R, U266 and U266LR7, and ANBL6 and ANBL6-BR cells measured by qRT-PCR. C, stable knockdown of LDHA restores the effect of bortezomib in ANBL6-bortezomib resistant. ANBL6 scramble and ANBL6-LDHA knockdown were incubated with bortezomib (5 and 10 nmol/L) for 24 hours and cell viability was evaluated by MTT. Graphs and bars represent the mean ± SD for cell viability in three independent experiments performed in four replicates. D, stable overexpression of LDHA induces resistance to bortezomib in MM1S cells. MM1S-scramble, HIF1A-overexpressed cells, and LDHA-overexpressed cells were incubated with bortezomib (5 and 10 nmol/L) for 24 hours and cell viability was evaluated by MTT. Graphs and bars represent the mean ± SD for cell viability in three independent experiments performed in four replicates.

MM1S the overexpression (OE) of HIF1A and LDHA induced resistant to bortezomib (Fig. 5D).

Taken together, these data suggest that HIF1A and LDHA are important targets for hypoxia-associated drug resistance and the reduction of LDHA increase the effect of bortezomib not only under hypoxic conditions but also in normoxic cells.

Discussion

Targeting cancer energy metabolism has been partly elusive because of the poor understanding of metabolic phenotypes of different cancers. One of the reasons for altered tumor metabolism is the physiologic stress that exists within the tumor. The tumor microenvironment suffers from hypoxia and the net result of hypoxia-inducible transcription factors activation is to shift energy production by increasing glycolysis and decreasing mitochondrial function (6, 7).

It is well established that hypoxia and consequently HIF1A activation is associated with metastasis in solid tumors and with poor patients outcome (26–28), but the metabolic-induced phenotype driven to drug resistance has been poorly explored mainly because the lack of understanding of cellular responses to inhibition of specific enzymes involved in energy metabolism. In this study, we demonstrate that altered metabolism has important implications for tumor cell growth and drug resistance.

We find that increased HIF1A-metabolic related targets such as HK2 and LDHA are present in plasma cells from newly diagnosed multiple myeloma patients and even more upregulated in relapsed multiple myeloma patients, highlighting the importance of elevated glucose metabolism in relapsed patients compared with newly diagnosed myeloma cells. This fact is further validated by the finding of a similar response and gene expression pattern in multiple myeloma cell lines under hypoxic conditions that persist even after bortezomib treatment and by the fact that both HIF1A and LDHA are overexpressed in multiple myeloma cell lines resistant to different treatments such as dexamethasone, melphalan, and bortezomib. On the basis of this, we hypothesized that metabolic alterations play a crucial role in drug

resistance in multiple myeloma. This is most critical in the MRD state when cells can survive in a hypoxic bone marrow niche after treatment with bortezomib and high-dose melphalan in stem cell transplantation, leading to ultimate recurrence of the disease.

In this study, we demonstrate that the increase of glycolytic metabolism results in increased lactate levels in multiple myeloma cells. Importantly, we show that increased glycolysis is not a consequence of the G_1 arrest that cells undergo after hypoxia conditions. Rather, hypoxia actively regulates cellular glucose metabolism by activation of glycolytic enzymes transcription as we demonstrate by GEP analysis and at the functional level by enzymatic assays. Thus, taken together, our study shows that increased glycolysis leads to chemotherapy resistance in multiple myeloma cells.

The role of dysregulated metabolism in therapeutic resistance has not been examined previously (12, 29–34). The ability to reduce chemoresistance through the inhibition of metabolic pathways would be an important research area to improve patient response to therapy. As a central energetic resource for the cell, glucose metabolism is quite complex. Many enzymes contribute to the glycolytic breakdown of glucose. In the glycolytic pathway, the first rate-limiting step is the transport of glucose across the plasma membrane through glucose transporters (GLUT family). GLUT family of proteins are often found upregulated in malignant cells (35). GLUT1 inhibitors, such as WZB117 and phloretin, decrease glucose uptake and display synergistic anticancer effects in lung, colon, and breast cancer as well as in leukemia *in vitro* (36, 37). Under hypoxia, the GLUT1 inhibitor, phloretin, significantly enhances daunorubicin effect and overcomes hypoxia-conferred drug resistance (38). Another key rate-limiting enzyme in glycolysis is HK, which has important roles in both glycolysis and apoptosis, and inhibitors of HK, such as 2-deoxyglucose (2-DG), 3-bromopyruvate (3-BrPA), and lonidamine (LND) are in preclinical and early-phase clinical trials (31). Although there are several reports showing that HK inhibitors enhance the drug response *in vitro* under normoxic conditions (39–41), there are no ongoing trials with HK inhibitors as a single agent due to the lack of response *in vivo* (42). Consistent with these data, we did not observe any effect in multiple myeloma cells treated with 2-DG, 3-BrPA, or LND under hypoxic conditions or in our *in vivo* model (data not shown). These findings together with the fact that bortezomib was able to decrease HK2 activity under hypoxic conditions and that our HK2 knockdown revealed a decrease in LDHA activity led us to hypothesize that the main enzyme to target in our hypoxia–drug-resistant model was LDHA. This hypothesis is further supported by the fact that both HIF1A and LDHA overexpression lead to drug resistance in MM1S, whereas LDHA knockdown sensitizes ANBL6 bortezomib-resistant cells to the effect of bortezomib. LDHA catalyzes the final step in the glycolytic pathway and has a critical role in tumor maintenance. LDHA contributes to paclitaxel/trastuzumab resistance in breast cancer (33, 34) and knockdown of LDHA increased mitochondrial respiration, decreased cellular ability to proliferate under hypoxic conditions, and suppressed tumorigenicity in tumor cells (43). In line with these data, our LDHA knockdown improves the effect of bortezomib in both normoxic and hypoxic conditions and showed a significant effect in our *in vivo* model.

Our *in vitro* experiments demonstrate that stable inhibition of HIF1A in multiple myeloma cells decreased proliferation and sensitized cells to the therapeutic effect of bortezomib. Stable depletion of HIF1A inhibited glycolysis and decreased lactate levels and this reduction of lactate remained at low levels even after the exposure to hypoxia. Reduction of HK2 and LDHA expression also increased the effect the bortezomib under hypoxic conditions; however, due to the LDHA reduction observed in our stable HK2 knockdown and due to the fact that hexokinase activity was also decreased in cells treated with bortezomib under hypoxic conditions, we proposed that LDHA could be one of the main targets to overcome drug resistance induced through hypoxia. Depletion of HIF1A and LDHA in multiple myeloma cells also restored drug sensitivity to therapeutic agents such as bortezomib *in vivo*. Multiple myeloma tumors with HIF1A knockdown clearly demonstrated a proliferative disadvantage compared with the scramble control tumors and a significant increase of survival in the bortezomib-treated group. LDHA knockdown significantly improved the response to bortezomib treatment; however, the overall survival in the nontreated group was similar to the scramble nontreated group. A possible explanation of the decreased proliferation in multiple myeloma tumor with HIF1A knockdown may relate to the downregulation of the entire HIF1A pathway that involves not only the effect on therapeutic response but also a decrease of proliferation and angiogenesis (28, 44, 45).

In summary, our studies reveal that regulation of tumor cell metabolism in multiple myeloma cells is essential to target drug resistance in multiple myeloma. We show that the metabolic phenotype in MRD cells induced by hypoxia leads to drug resistance through HIF1A and that specific regulation of HIF1A or LDHA can restore sensitivity to therapeutic agents such as bortezomib and melphalan and can also inhibit tumor growth induced by altered metabolism.

Disclosure of Potential Conflicts of Interest

A.C. Kimmelman receives speakers bureau honoraria from Agios and US oncology and is a consultant/advisory board member for Astellas, Forma therapeutics, and Gilead. I.M. Ghobrial is an advisory board member for Millennium/Takeda, Bristol-Myers Squibb, Celgene, and Onyx/Amgen. No potential conflicts of interest were disclosed by the other authors.

Authors' Contributions

Conception and design: P. Maiso, I.M. Ghobrial
Development of methodology: P. Maiso, Y. Mishima, J.M. Asara, I.M. Ghobrial
Acquisition of data (provided animals, acquired and managed patients, provided facilities, etc.): P. Maiso, M. Moschetta, Y. Aljawai, J.M. Asara, I.M. Ghobrial
Analysis and interpretation of data (e.g., statistical analysis, biostatistics, computational analysis): P. Maiso, M. Moschetta, Y. Aljawai, J.M. Asara, A.C. Kimmelman, I.M. Ghobrial
Writing, review, and/or revision of the manuscript: P. Maiso, A.M. Roccaro, A.C. Kimmelman, I.M. Ghobrial
Administrative, technical, or material support (i.e., reporting or organizing data, constructing databases): Y. Aljawai, I.M. Ghobrial
Study supervision: P. Maiso, I.M. Ghobrial
Other (designed and performed the *in vitro* and *in vivo* functional experiments): D. Huynh
Other (performed *in vitro* assays): A. Sacco

Grant Support

This work was supported in part by EHA (European Hematology Association), SPORE P50 CA100707, NIH R01CA154648, Leukemia and Lymphoma Society, and Miguel Servet program from Instituto de Salud Carlos III.

The costs of publication of this article were defrayed in part by the payment of page charges. This article must therefore be hereby marked *advertisement* in accordance with 18 U.S.C. Section 1734 solely to indicate this fact.

Received November 19, 2014; revised February 7, 2015; accepted February 27, 2015; published OnlineFirst March 13, 2015.

References

1. Gatenby RA, Gillies RJ. Why do cancers have high aerobic glycolysis? Nat Rev Cancer 2004;4:891–9.
2. Racker E. History of the Pasteur effect and its pathobiology. Mol Cell Biochem 1974;5:17–23.
3. Semenza GL, Artemov D, Bedi A, Bhujwalla Z, Chiles K, Feldser D, et al. `The metabolism of tumours': 70 years later. Novartis Found Symp 2001; 240:251–60.
4. Warburg O. On respiratory impairment in cancer cells. Science 1956; 124:269–70.
5. Warburg O, Wind F, Negelein E. The metabolism of tumors in the body. J Gen Physiol 1927;8:519–30.
6. Denko NC. Hypoxia, HIF1 and glucose metabolism in the solid tumour. Nat Rev Cancer 2008;8:705–13.
7. Milosevic M, Fyles A, Hedley D, Hill R. The human tumor microenvironment: invasive (needle) measurement of oxygen and interstitial fluid pressure. Semin Radiat Oncol 2004;14:249–58.
8. Chi JT, Wang Z, Nuyten DS, Rodriguez EH, Schaner ME, Salim A, et al. Gene expression programs in response to hypoxia: cell type specificity and prognostic significance in human cancers. PLoS Med 2006;3:e47.
9. Vengellur A, Woods BG, Ryan HE, Johnson RS, LaPres JJ. Gene expression profiling of the hypoxia signaling pathway in hypoxia-inducible factor 1alpha null mouse embryonic fibroblasts. Gene Expr 2003;11: 181–97.
10. Kaelin WG Jr, Ratcliffe PJ. Oxygen sensing by metazoans: the central role of the HIF hydroxylase pathway. Mol Cell 2008;30:393–402.
11. Semenza GL. HIF-1: upstream and downstream of cancer metabolism. Curr Opin Genet Dev 2010;20:51–6.
12. Tennant DA, Duran RV, Gottlieb E. Targeting metabolic transformation for cancer therapy. Nat Rev Cancer 2010;10:267–77.
13. Maiso P, Carvajal-Vergara X, Ocio EM, Lopez-Perez R, Mateo G, Gutierrez N, et al. The histone deacetylase inhibitor LBH589 is a potent antimyeloma agent that overcomes drug resistance. Cancer Res 2006; 66:5781–9.
14. Maiso P, Liu Y, Morgan B, Azab AK, Ren P, Martin MB, et al. Defining the role of TORC1/2 in multiple myeloma. Blood 2011;118:6860–70.
15. Schaefer CF, Anthony K, Krupa S, Buchoff J, Day M, Hannay T, et al. PID: the pathway interaction database. Nucleic Acids Res 2009;37:D674–9.
16. Chng WJ, Kumar S, Vanwier S, Ahmann G, Price-Troska T, Henderson K, et al. Molecular dissection of hyperdiploid multiple myeloma by gene expression profiling. Cancer Res 2007;67:2982–9.
17. Mulligan G, Mitsiades C, Bryant B, Zhan F, Chng WJ, Roels S, et al. Gene expression profiling and correlation with outcome in clinical trials of the proteasome inhibitor bortezomib. Blood 2007;109:3177–88.
18. Luo B, Groenke K, Takors R, Wandrey C, Oldiges M. Simultaneous determination of multiple intracellular metabolites in glycolysis, pentose phosphate pathway and tricarboxylic acid cycle by liquid chromatography-mass spectrometry. J Chromatogr A 2007;1147:153–64.
19. Finley LW, Carracedo A, Lee J, Souza A, Egia A, Zhang J, et al. SIRT3 opposes reprogramming of cancer cell metabolism through HIF1alpha destabilization. Cancer Cell 2011;19:416–28.
20. Hirschhaeuser F, Sattler UG, Mueller-Klieser W. Lactate: a metabolic key player in cancer. Cancer Res 2011;71:6921–5.
21. Patra KC, Wang Q, Bhaskar PT, Miller L, Wang Z, Wheaton W, et al. Hexokinase 2 is required for tumor initiation and maintenance and its systemic deletion is therapeutic in mouse models of cancer. Cancer Cell 2013;24:213–28.
22. Wheaton WW, Chandel NS. Hypoxia. 2. Hypoxia regulates cellular metabolism. Am J Physiol Cell Physiol 2011;300:C385–93.
23. Wilson WR, Hay MP. Targeting hypoxia in cancer therapy. Nat Rev Cancer 2011;11:393–410.
24. Ivan M, Kondo K, Yang H, Kim W, Valiando J, Ohh M, et al. HIFalpha targeted for VHL-mediated destruction by proline hydroxylation: implications for O2 sensing. Science 2001;292:464–8.
25. Ader I, Brizuela L, Bouquerel P, Malavaud B, Cuvillier O. Sphingosine kinase 1: a new modulator of hypoxia inducible factor 1alpha during hypoxia in human cancer cells. Cancer Res 2008;68:8635–42.
26. Shin DH, Chun YS, Lee DS, Huang LE, Park JW. Bortezomib inhibits tumor adaptation to hypoxia by stimulating the FIH-mediated repression of hypoxia-inducible factor-1. Blood 2008;111:3131–6.
27. Erler JT, Bennewith KL, Nicolau M, Dornhofer N, Kong C, Le QT, et al. Lysyl oxidase is essential for hypoxia-induced metastasis. Nature 2006;440: 1222–6.
28. Erler JT, Bennewith KL, Cox TR, Lang G, Bird D, Koong A, et al. Hypoxia-induced lysyl oxidase is a critical mediator of bone marrow cell recruitment to form the premetastatic niche. Cancer Cell 2009;15:35–44.
29. Birsoy K, Sabatini DM, Possemato R. Untuning the tumor metabolic machine: targeting cancer metabolism: a bedside lesson. Nat Med 2012; 18:1022–3.
30. Dang CV, Hamaker M, Sun P, Le A, Gao P. Therapeutic targeting of cancer cell metabolism. J Mol Med 2011;89:205–12.
31. El Mjiyad N, Caro-Maldonado A, Ramirez-Peinado S, Munoz-Pinedo C. Sugar-free approaches to cancer cell killing. Oncogene 2011;30:253–64.
32. Hamanaka RB, Chandel NS. Targeting glucose metabolism for cancer therapy. J Exp Med 2012;209:211–5.
33. Zhao Y, Liu H, Liu Z, Ding Y, Ledoux SP, Wilson GL, et al. Overcoming trastuzumab resistance in breast cancer by targeting dysregulated glucose metabolism. Cancer Res 2011;71:4585–97.
34. Zhou M, Zhao Y, Ding Y, Liu H, Liu Z, Fodstad O, et al. Warburg effect in chemosensitivity: targeting lactate dehydrogenase-A re-sensitizes taxol-resistant cancer cells to taxol. Mol Cancer 2010;9:33.
35. Macheda ML, Rogers S, Best JD. Molecular and cellular regulation of glucose transporter (GLUT) proteins in cancer. J Cell Physiol 2005; 202:654–62.
36. Liu Y, Cao Y, Zhang W, Bergmeier S, Qian Y, Akbar H, et al. A small-molecule inhibitor of glucose transporter 1 downregulates glycolysis, induces cell-cycle arrest, and inhibits cancer cell growth *in vitro* and *in vivo*. Mol Cancer Ther 2012;11:1672–82.
37. Monti E, Gariboldi MB. HIF-1 as a target for cancer chemotherapy, chemosensitization and chemoprevention. Curr Mol Pharmacol 2011;4: 62–77.
38. Cao X, Fang L, Gibbs S, Huang Y, Dai Z, Wen P, et al. Glucose uptake inhibitor sensitizes cancer cells to daunorubicin and overcomes drug resistance in hypoxia. Cancer Chemother Pharmacol 2007;59:495–505.
39. Kurtoglu M, Gao N, Shang J, Maher JC, Lehrman MA, Wangpaichitr M, et al. Under normoxia, 2-deoxy-D-glucose elicits cell death in select tumor types not by inhibition of glycolysis but by interfering with N-linked glycosylation. Mol Cancer Ther 2007;6:3049–58.
40. Maher JC, Krishan A, Lampidis TJ. Greater cell cycle inhibition and cytotoxicity induced by 2-deoxy-D-glucose in tumor cells treated under hypoxic vs aerobic conditions. Cancer Chemother Pharmacol 2004;53: 116–22.
41. Pelicano H, Martin DS, Xu RH, Huang P. Glycolysis inhibition for anticancer treatment. Oncogene 2006;25:4633–46.
42. Maschek G, Savaraj N, Priebe W, Braunschweiger P, Hamilton K, Tidmarsh GF, et al. 2-deoxy-D-glucose increases the efficacy of adriamycin and paclitaxel in human osteosarcoma and non-small cell lung cancers *in vivo*. Cancer Res 2004;64:31–4.
43. Fantin VR, St-Pierre J, Leder P. Attenuation of LDH-A expression uncovers a link between glycolysis, mitochondrial physiology, and tumor maintenance. Cancer Cell 2006;9:425–34.
44. Martin SK, Diamond P, Gronthos S, Peet DJ, Zannettino AC. The emerging role of hypoxia, HIF-1 and HIF-2 in multiple myeloma. Leukemia 2011;25:1533–42.
45. Zhang Y, Li M, Yao Q, Chen C. Recent advances in tumor hypoxia: tumor progression, molecular mechanisms, and therapeutic implications. Med Sci Monit 2007;13:RA175–80.